Journal of Applied Fluid Mechanics, Vol. 17, No. 12, pp. 2775-2790, 2024.
Available online at www.jafmonline.net, ISSN 1735-3572, EISSN 1735-3645.
https://doi.org/10.47176/jafm.17.12.2594

Simulation Study on Impacts of Viaduct Height on Pollutant Dispersion in Street Canyons Using LES and RANS Models

R. Xu[1], T. Chen[1], Y. X. Fu[1], J. C. Chen[2] and Y. H. Liu[1†]

[1] *Guangdong Provincial Key Laboratory of Intelligent Transportation System, School of Intelligent Systems Engineering, Shenzhen Campus of Sun Yat-sen University, Shenzhen, Guangdong, 518107, China*
[2] *School of Civil and Transportation Engineering, Guangdong University of Technology, Guangzhou, Guangdong, 510006, China*

†*Corresponding Author Email: liuyh3@mail.sysu.edu.cn*

ABSTRACT

To assess the impact of different heights of the viaduct on air pollutant dispersion and the prediction accuracy of pollutant concentration in urban street canyons, simulation results based on LES and RANS models are analyzed. The presence of a viaduct generated a poorly ventilated region underneath it, and RANS significantly underestimated the wind speed and grossly overestimated the pollutant concentration. LES gives better results for the flow pattern, distribution of turbulent kinetic energy and mean pollutant concentration. With a fluctuation of less than 15% of the pollutant concentration, both RANS and LES cases show that an increase in the viaduct height has a weak impact on the concentration of pollutants in most areas of the canyon except windward, and cases with a viaduct height of 0.75H had the lowest predicted pollutant concentration relative to other cases with a viaduct as a result of better ventilation. In addition, LES found a subregion of pollutant accumulation above the ground, but RANS did not.

Article History

Received January 28, 2024
Revised April 26, 2024
Accepted June 1, 2024
Available online October 2, 2024

Keywords:

Street canyon
Viaduct
Pollution distribution
Large eddy simulation
Computational Fluid Dynamic

1. INTRODUCTION

Owing to increasing vehicle ownership and rapid urbanization, traffic exhaust has become one of the most important sources of urban air pollution (Pu & Yang, 2014). Especially in densely built areas, urban street canyons (referred to as "canyons" in the following text) formed by spaces between buildings weaken the ability of pollutant dispersion by reducing natural ventilation (Li et al., 2006; Tominaga & Stathopoulos, 2013). Moreover, viaducts are commonly used in many cities to increase the traffic capacity in places with heavy traffic, which could lead to a more complex pollutant dispersion mechanism and more severe air pollution. Residents and pedestrians nearby may be at increased health risks of being hospitalized for a range of problems, such as lung and heart diseases, following long- and short-term exposure to heavy air pollution (Zhou et al., 2013; Kim et al., 2015; Liu et al., 2020;). Therefore, investigations of pollutant dispersion processes in canyons have become a hotspot and frontier issue in environmental research.

To date, numerous studies on air pollutant dispersion in canyons have been based on three methods: outdoor field measurements (Eliasson et al., 2006; Kumar et al., 2009), controlled laboratory experiments (Kastner-Klein & Plate, 1999; Chang & Meroney, 2003; Gromke & Ruck, 2009) and numerical simulations based on computational fluid dynamics (CFD) (So et al., 2005; Toparlar et al., 2017; Zhang et al., 2018).

Most of these studies have focused on the effects of several key parameters, including the AR of canyons-(Li et al., 2008; Ng & Chau, 2014; He et al., 2017; Chew et al., 2018a; Hang et al., 2018), building height variation (Gu et al., 2011; Hang et al., 2012; Kikumoto & Ooka, 2012), roof shape (Takano & Moonen, 2013; Bouarbi et al., 2016; Llaguno-Munitxa et al., 2017; Allegrini, 2018), wind conditions (Jon et al., 2023a, b), atmospheric temperature stratification (Huang et al., 2023) and urban vegetation (Oachim & Ichhorn, 2004; Gromke & Ruck, 2007; Salim et al., 2011a). In general, the main form of canyons is determined by their H, L and W. When L/W is greater than 20, an isolated 3D canyon with H/W=1 can be simplified and analyzed as a 2D canyon (Mei et al., 2019). For incoming winds perpendicular to the street, the flow regimes in 2D canyons are primarily determined by aspect ratios: at H/W<0.3, a recirculating flow is formed on the leeward side; as H/W increases, the wake from the upwind building starts to disrupt the recirculating flow, and then the wake.

NOMENCLATURE

H	building height	L	street length
W	street width	AR	building height/street width
SKE	standard k-ε	RANS	Reynolds-Averaged Navier–Stokes
LES	Large Eddy Simulation	SF_6	sulfur hexafluoride
WT	Wind Tunnel	Y	mass fraction of pollutant in air
δ	depth of boundary layer	u_*	friction velocity
Q	emission intensity	c^+	normalized concentration
L	road length	C	observed concentration
J	diffusion flux of pollutant in air	U_{ref}	wind velocity at reference height
TKE	Turbulent Kinetic Energy	κ	Von Kármán constant, 0.4
D	mass diffusion coefficient for pollutant in mixture		

An interference regime can be observed when the H/W is between 0.3 and 0.7. Furthermore, the skimming flow regime is expected with one single main vortex in the canyon at 0.7<H/W<1.5. In a deep canyon (H/W>1.5), one or more vortices are formed in terms of the Reynolds flow number (Chew et al., 2018a). It has been shown that deeper canyons weaken the ventilation efficiency and consequently cause heavier air pollution inside the canyons (Li et al., 2008; Kikumoto & Ooka, 2012; Ng & Chau, 2014; He et al., 2017; Chew et al., 2018a; Hang et al., 2018). Additionally, the flow and air pollutant dispersion mechanisms are also significantly influenced by the other crucial variables. For example, the presence of trees reduces the ventilation and wind velocity while increasing the concentration of pollutants on the leeward side. As the tree crown diameter increases, the concentration on the leeward side increases (Gromke & Ruck, 2007). By contrast, other parameters, including building height variations and roof shape, may produce much greater vertical ventilation flow rates and improve the air quality in canyons (Gu et al., 2011; Hang et al., 2012; Kikumoto & Ooka, 2012). In particular, the presence of a viaduct spills the air flow, greatly impeding the dispersion of pollutants in canyons. Consequently, studies investigating air pollutant dispersion in canyons with a viaduct have gained increasing attention.

An overview of CFD studies on the impacts of viaduct settings on air pollutant dispersion in canyons was presented, including the use of numerical methods, turbulence models, street aspect ratio settings, and viaduct heights in Table 1.

Jian Hang and his colleagues completed a series of studies on the impacts of viaduct settings on air quality in both 2D (Hang et al., 2016, 2019; Zhang et al., 2019) and 3D (Hang et al., 2017; He et al., 2017; Hang et al., 2018) street canyons. They indicated that a viaduct can be viewed as an addition of a new horizontal surface that reduces the effective aspect ratio in the canyon. Their extensive studies revealed that viaduct settings affect flow patterns and pollutant exposure in regular 2D canyons (H/W=0.5~1) more than in deep canyons (H/W=5~6), and the presence of viaducts affects the pollutant concentration distribution characteristics in 3D canyons. In addition, field measurements (Joerger & Pryor, 2018) and numerical simulations (Qin et al., 2018) from previous research have verified the major impact of urban viaducts on air pollutant dispersion. The effect of different viaduct height settings on pollution flow and concentration in canyons has also been studied by researchers. C. Zhang et al., 2012 compared the performance of the SKE model with respect to the viaduct width and height. They concluded that the width of the viaduct has a more significant impact on pollution dispersion than does the height at which it is placed, while the height has a greater influence on flow patterns (Zhou et al., 2013; Kim et al., 2015; Li et al., 2018; Liu et al., 2020), which they discovered by setting four different heights in a deep canyon.

In addition, based on the RNG k-ε turbulence model, (Ding et al., 2019) built a 2D ideal canyon with two different roof shapes and a viaduct to study air flow and pollutant transportation. They found that as the viaduct increases to 0.71~0.988H, the vortex above the viaduct changes into a main clockwise vortex, and pollutants build up on the windward side.

Table 1 Overview of CFD studies in street canyons considering different viaduct heights

Ref.	Turb. model	Dim.	AR	The viaduct height/H	WT
(Zhang et al., 2012)	RANS SKE	2D	1	0.25, 0.5, 0.75	-
(Li et al., 2018)	RANS SKE	2D	1	0.4, 0.6, 0.8, 1	-
(Zhang et al., 2019)	RANS SKE	3D	2	0.42, 0.75	No viaduct
(Ding et al., 2019)	RANS RNG	2D	1	0.2, 0.47, 0.6, 0.875, 1.2	0.6H, 0.9H
(Ming et al., 2022)	RANS SKE	2D	1	0.4, 0.6, 0.8, 1	-
(Meroney et al., 1996)	-	-	-	-	No viaduct
(Kastner-Klein & Plate, 1999)	-	-	-	-	No viaduct
(Chang & Meroney, 2003)	RANS	3D	1, 4, 6	-	No viaduct
(Gromke, 2013)	-	-	-	-	No viaduct

Ref.: References. Dim.: Simulation dimension, 2D or 3D.

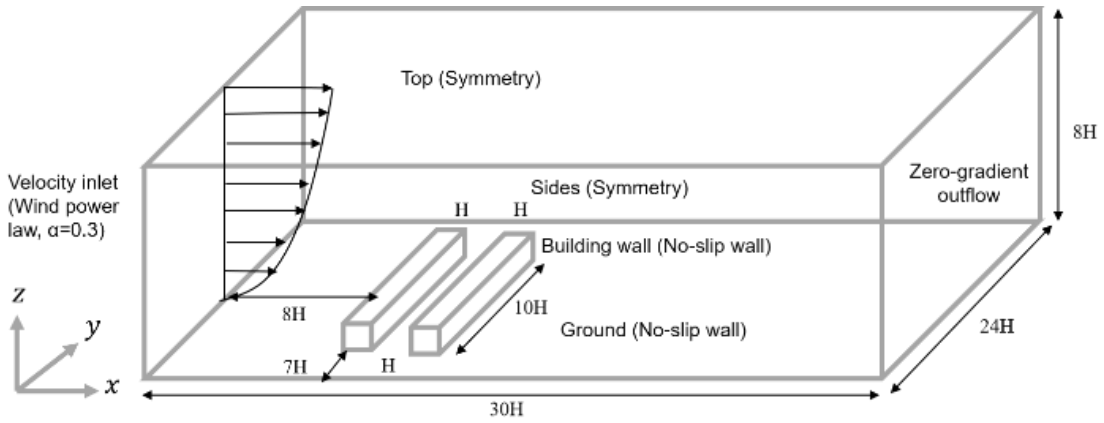

Fig. 1 CFD setups for the boundary conditions and computational domain

Only a relatively limited number of publications have reported studies about the impact of different viaduct heights, and including both RANS and LES. In fact, few studies researchers perform their simulations by using the LES method, which is often not a viable option due to its great computational demand (Wong & Liu, 2014; Li et al., 2016). However, a variety of studies comparing steady-state RANS and LES methods have shown that LES modeling can better reproduce the horizontal diffusion of pollutant concentrations and represent secondary flow topological features because of its ability to address unsteady and intermittent fluctuations in the flow fields in canyons without viaducts (Li et al., 2008; Gousseau et al., 2011; Tominaga & Stathopoulos, 2013; Chew et al., 2018b; Hayati et al., 2019), which cannot be obtained from RANS. In general, RANS methods are unable to simulate such complex flows, while LES methods perform well in predicting complex turbulent vortices (Breuer et al., 2003; Shao & Zhang, 2006).

The overview of CFD studies in street canyons with a viaduct clearly demonstrates that there is currently not enough exploration of this issue based on the LES model. The effect of the viaduct height on pollution dispersion is nearly limited to 2D numerical simulations. Compared to 2D simulation, 3D simulation is able to provide spatial results rather than a flat surface, thus truly restoring the flow field and pollution field inside the canyon. Moreover, comparisons of the performances of several CFD methods on the flow and removal of pollutants are still limited. Source height has a major impact on street-level concentrations of pollutants (Chatzimichailidis et al., 2019). Viaducts enhance turbulence instability, and the sources of pollution they carry at different heights from the ground may affect the distribution of pollution. Discrepancies between the prediction accuracy of RANS and LES in canyons within a viaduct setting may be significantly enlarged. However, quantitative analyses of the impact of the viaduct setting at different heights on flow and pollution dispersion in canyons are still lacking. Based on LES simulation results, some important information regarding instantaneous fluctuations in flow and concentration could be better understood. Therefore, the objective of this work is to compare 3D steady RANS and LES modeling of the impacts of viaduct settings at different heights on air pollutant flow and dispersion in a typical canyon (H/W=1) and to analyze the relationship between pollutant removal and the flow field. Targeted cases were designed to compare the results between the RANS and LES methods, and a detailed analysis of the effects of the viaduct height is given. This approach may help us determine which simulation approach is better at forecasting air pollutant dispersion processes and gain a better understanding of pollution dispersion mechanisms in canyons with viaducts at different heights.

The remainder of this paper is organized as follows. The methodology, including different physical and mathematical models and corresponding numerical settings, is described in Section 2. The modeling results and discussion are presented in Section 3. Lastly, conclusions are provided in Section 4.

2. MODEL DESCRIPTION

2.1. Street Canyon Model and Boundary Conditions

An idealized 3D street canyon model (W/H=1) was built based on the wind tunnel experimental studies of (Gromke & Ruck, 2007). The concentration data are available on the website www.codasc.de (Gromke, 2013). The model scale is 1:150 for a street canyon with a length of L=180 m and height of H=18 m. The computational domain is a cube of x=30H, y=24H, and z=8H, as shown in Fig. 1. The flow entry is configured to the inlet boundary condition when it is 8H away from the closest building. The outlet at a distance of 19H from the upstream obstacles was defined as the outflow boundary condition. For the building walls, viaducts and floors, non-slip conditions were applied. Lastly, symmetry conditions were imposed on the two sides and the top of the domain to guarantee parallel flow.

To investigate the impacts of the viaduct settings on flow and pollution dispersion in canyons, an idealized viaduct model with width W_v=0.5H and thickness 0.077H was constructed along the canyons at height h_v above the ground. In this study, a total of 8 cases were combined with different viaduct settings (different viaduct heights h_v=0, 0.5H, 0.75H and 1H) using steady RANS or LES, as shown in Table 2 and Fig. 2. The two cases with h_v=0 indicate no viaduct in the canyon. Noise barriers and piers

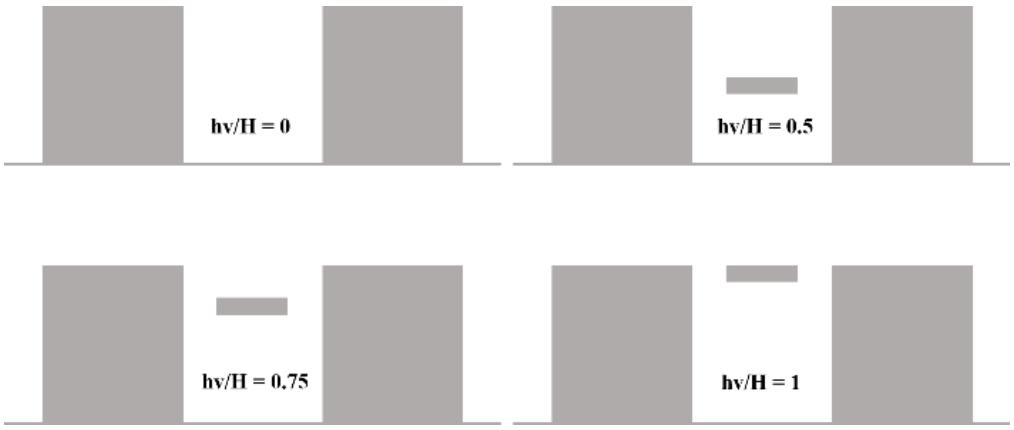

Fig. 2 Sketches (a slice in the x-z plane) of street canyons with viaducts at different heights h_v above the ground. h_v/H=0 also indicates a canyon without a viaduct

Table 2 Setups for 8 case studies

Index	Model	Viaduct height	Index	Model	Viaduct height
Case1	RANS	0	Case5	LES	0
Case2	RANS	0.5H	Case6	LES	0.5H
Case3	RANS	0.75H	Case7	LES	0.75H
Case4	RANS	1H	Case8	LES	1H

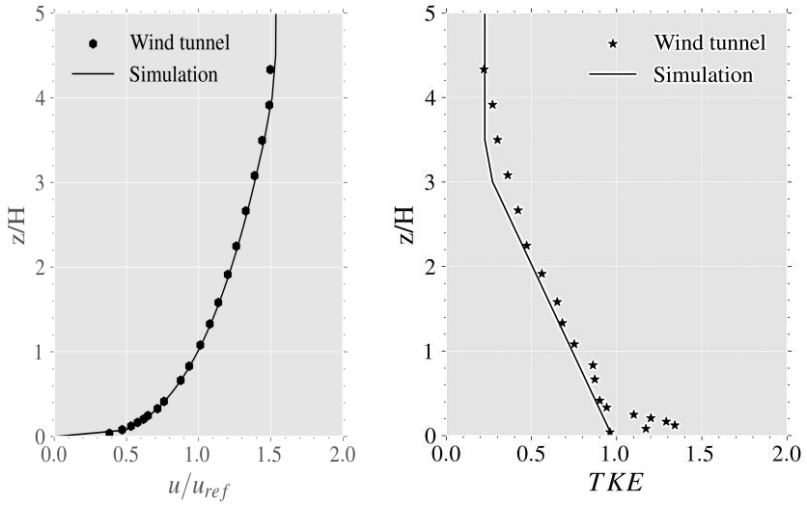

(a) (b)

Fig. 3 Inlet profiles of the (a) velocity magnitude and (b) TKE

were ignored in this study to simplify our models significantly so that we could focus on primary factors.

According to wind tunnel tests (Gromke & Ruck, 2007), the velocity inlet profile satisfies

$$u_z = 4.7*\left(z/0.12\right)^{0.3} \tag{1}$$

The equations for the dissipation rate (Eq. 2) and TKE, (Eq. 3) of the velocity-inlet profiles are described as

$$\dot{o} = u_*^3 / \kappa z*\left(1-z/\delta\right) \tag{2}$$

and

$$k = u_*^2 / \sqrt{(C_\mu)}*\left(1-z/\delta\right) \tag{3}$$

where u_z is the velocity at vertical height z, k is the TKE, ε is the dissipation rate, and δ is approximately 0.5 m. Fig. 3 shows the inlet profiles of the velocity magnitude and TKE for the wind tunnel experiment and simulation.

Table 3 gives the value of u_* and the constant values of the other equations. The constants in Table 3 refer to previous studies (Salim et al., 2011a; Salim & Ong, 2013).

Table 3 The values of the constants in the equations

Constant	Value	Equation
u_*	0.54 m/s	(3)
κ	0.4	(3)
C_μ	0.09	(3), (7)
σ_k	1.00	(7)
σ_ϵ	1.30	(7)
$C_{1\varepsilon}$	1.44	(8)
$C_{2\epsilon}$	1.92	(8)

The concentration data are given in normalized form according to

$$c^+ = CU_{ref} HL / Q \tag{4}$$

where c^+ represents the normalized concentration and Q/L denotes the emission intensity per unit length.

2.2. Flow Modeling

Considering the characteristics of low wind speeds in canyons and in referring to urban canyon studies (Salim et al., 2011a, b), we use the incompressible N-S (Navier-Stokes) equation for fluid modeling. The steady-state RANS turbulence models have been widely employed to produce numerical predictions of turbulent flow in street canyon-scale environments. Eqs. (5) and (6) are the continuity equation and the momentum equation, respectively.

$$\partial \bar{u}_i / \partial x_i = 0 \tag{5}$$

and

$$\bar{u}_j \frac{\partial \bar{u}_i}{\partial x_j} = -\frac{1}{\rho}\frac{\partial \bar{p}}{x_i} + \mu \frac{\partial \bar{u}_i}{\rho \partial x_j^2} - \frac{\partial \overline{u_{i'} u_{j'}}}{\partial x_j^2} \tag{6}$$

Eqs. (7) and (8) are transport equations for k and ϵ, respectively.

$$\frac{\partial(\rho k u_i)}{\partial x_i} = \frac{\partial}{\partial x_j}[(\mu + \frac{\mu_t}{\sigma_k})\frac{\partial k}{\partial x_j}] + G_k - \rho \dot{o} \tag{7}$$

and

$$\frac{\partial(\rho \dot{o} u_i)}{\partial x_i} = \frac{\partial}{\partial x_j}[(\mu + \frac{\mu_t}{\sigma_{\dot{o}}})\frac{\partial \dot{o}}{\partial x_j}] + \frac{C_{1\dot{o}}\dot{o}}{k} G_k - C_{2\dot{o}}\rho \frac{\dot{o}^2}{k} \tag{8}$$

where $\bar{}$ denotes time averaging and $\bar{u}$ and u' are the mean velocity and fluctuating velocity components, respectively. ρ is a constant and represents fluid density, $\bar{p}$ is the mean pressure, μ is the fluid kinematic viscosity, and $\sigma_k, \sigma_\varepsilon, C_{1\varepsilon}$ and $C_{2\varepsilon}$ serve as the default closure constants.

In this study, the SKE model has the best performance in this scene according to (Zheng & Yang, 2021), so it is adopted to solve the RANS mean solution. A second-order upwind scheme is used for the transport equations, and SIMPLE is employed for solving the pressure-velocity field. For all the solving parameters, the residual is set at 1×10^{-5}.

The LES method is increasingly used as a tool for studying urban air pollution. The LES equation can be described as a spatial filtering operation of the N-S equations,

$$\partial \tilde{u}_i / \partial x_i = 0 \tag{9}$$

and

$$\frac{\partial \tilde{u}_i}{\partial t} + \tilde{u}_j \frac{\partial \tilde{u}_i}{\partial x_j} = -\frac{1}{\rho}\frac{\partial \tilde{p}}{x_i} + \frac{\partial}{\partial x_j}(\mu \frac{\partial \overline{u_i}}{\partial x_j}) - \frac{\partial \tau_{ij}}{\partial x_j} \tag{10}$$

where the tilde ~ indicates spatial filtering and the SGS turbulent stress term is

$$\tau_{ij} = \rho \overline{u_i u_j} - \rho \tilde{u}_i \tilde{u}_j \tag{11}$$

which is modeled by choosing the dynamic SGS (Smagorinsky-Lilly Sub-grid Scale) model according to previous studies (Salim, et al., 2011a, b; Moonen et al., 2013; Salim & Ong, 2013). In addition, the momentum is solved by a bounded central difference scheme, while the species transport equations are solved by using a second-order time-advancement and a second-order upwind algorithm. The pressure-velocity couples are solved by SIMPLE. All LES cases converge at 1×10^{-3} for the convergence residual of the time step, and the dimensionless time step length is set to 2.5×10^{-3} with reference to previous studies (Salim et al., 2011a; Salim & Ong, 2013). The LES results averaged over 15000 time steps, corresponding to 37.5 s of flow time. To ensure that the averaging time is long enough to obtain statistically steady results, the mean velocity at different locations inside the canyon was monitored over time. (Salim et al., 2011a, b) reported that steady-state conditions were achieved at 30 s under the same boundary conditions according to the LES model.

2.3. Dispersion Modeling

The dispersion of pollutants is modeled by using the advection-diffusion method as Eq.(12),

$$J = -(\rho D + \mu_t / Sc_t)\nabla Y \tag{12}$$

where ρ is the mixture density, μ_t is the turbulent eddy viscosity, and Sc_t is the turbulent Schmidt constant. The exhaust emission is modeled by putting two line sources on the ground and one additional line source on the viaduct. Each line source is simulated with SF_6 discharged at a rate of $Q = 10g/s$, acting as the pollutant species. Figure 4 shows the settings of the line source on

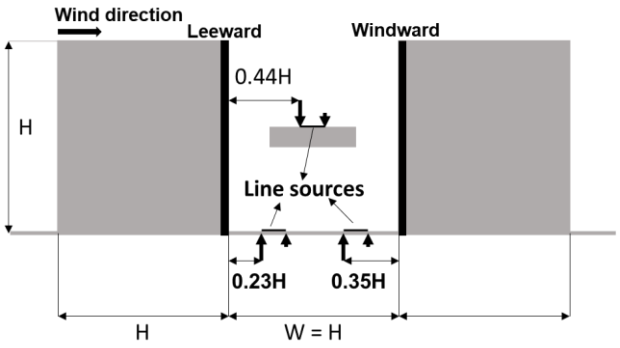

Fig. 4 Sketches of the positions of the line sources, windward wall and leeward wall

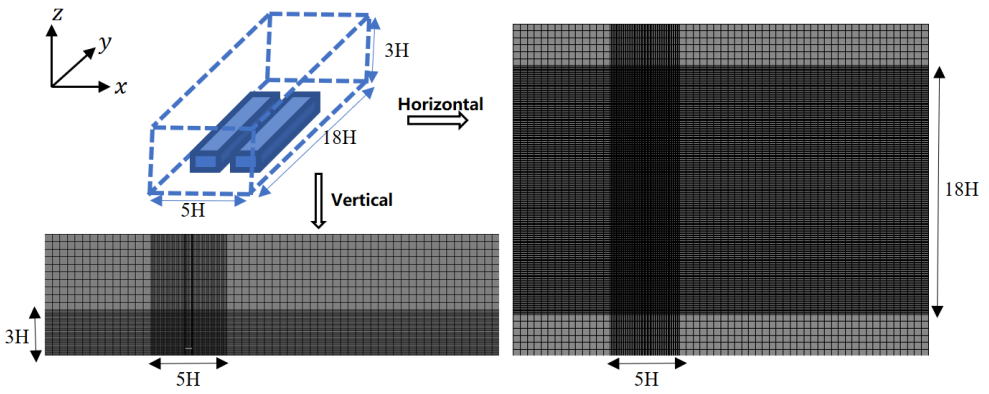

Fig. 5 Grid arrangement in the CFD validation cases

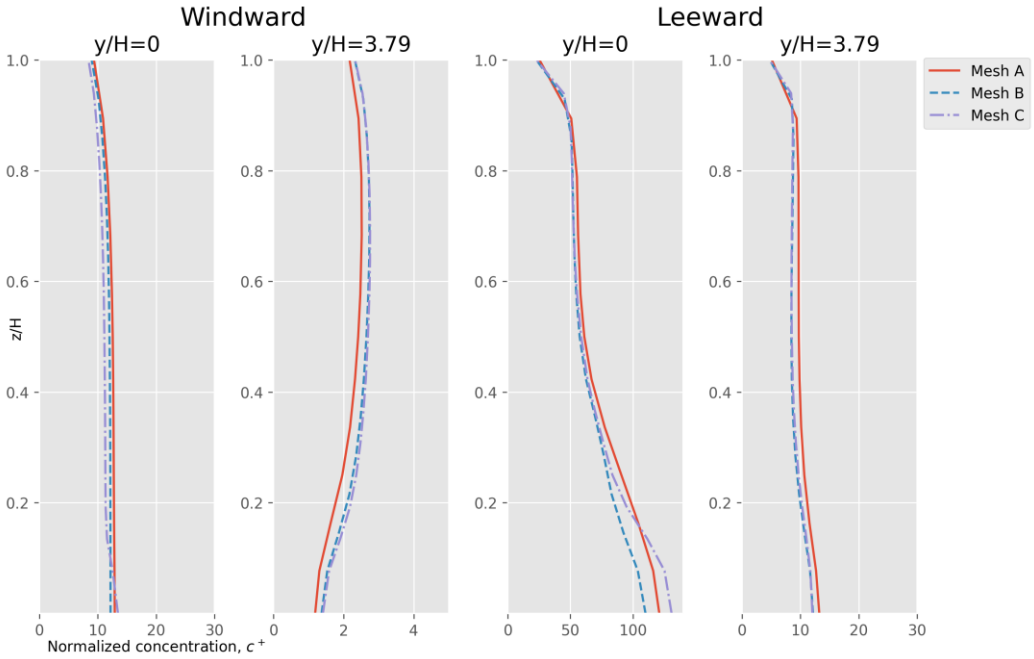

Fig. 6 Grid sensitivity analysis: comparison of mean normalized concentration profiles at different locations (y/H=0 and 3.79) close to the leeward and windward sides

the ground and viaduct as well as the location on the windward and leeward sides.

2.4. Model Validation

Grid sensitivity analysis All the cases are performed in the CFD software Fluent, which has been frequently employed in urban microscale environmental research. Fig. 5 shows the densified area and the strategy for dividing grids. Three grid arrangements were tested for RANS with the SKE model. The coarse, medium and fine grids contained 795536 cells with a minimum $\Delta x = 0.1H$, 1426620 cells with a minimum $\Delta x = 0.077H$, and 1978140 cells with a minimum $\Delta x = 0.067H$. These three grid sizes are the same as those in the study by (Salim et al., 2011a). An analysis of the grid sensitivity analysis by means of the normalized concentration of SF_6 at different vertical locations along the leeward and windward sides (at each wall: y/H=3.79 and y/H=0) is shown in Fig. 6. Compared to Mesh A, Mesh B provided more accurate computations when using RANS. The simulation results of fine cells in Mesh C did not significantly differ from those in Mesh B (0.72%); hence, the increase in cost was not unexpected.

The LES simulation is conducted on coarse and medium grids to reduce the computational cost since the minimum cell size for Mesh B is 0.077H, which is considered the most suitable mesh and was verified by (Salim et al., 2011b). The comparisons also show that the Mesh B arrangement possesses credible numerical accuracy in predicting airflow and pollutant filed. Therefore, Mesh B is adopted for further case studies of both the RANS and LES considering both the numerical accuracy and computational demand efficiency.

It should be noted that the y^+ ranged from 30 to 300 at wall surfaces in the RANS, while the value was lower than 10 in most regions of wall surfaces in the LES Sc_t for modeling dispersion in this work was determined to be 0.7 based on historical

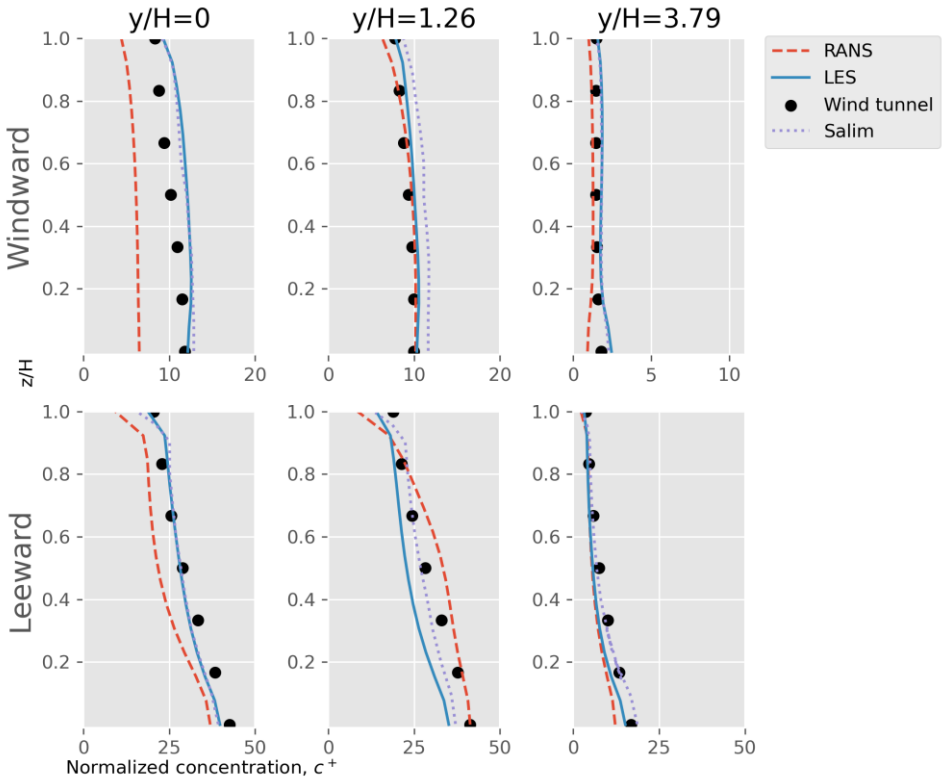

Fig. 7 Mean normalized concentration at three different locations (y/H=0, 1.26 and 3.79) on the leeward and windward sides. The "RANS" and "LES" were obtained from the present cases without viaducts

Table 4 Metrics for statistical performance in the validation case

Metric	Leeward		Windward		Acceptance criteria
	RANS	LES	RANS	LES	
NMSE	0.037	0.026	0.161	0.021	<1.5
FB	0.087	0.114	0.234	0.117	[-0.3,0.3]

studies (Zheng & Yang, 2021), which is consistent with the experimental data.

Concentration validation for the canyons Further pollutant concentration validation was completed by performing comparisons with wind tunnel data (Gromke, 2013). The mean normalized concentrations at three locations on the leeward and windward sides from case 1 (RANS without viaduct) and case 5 (LES without viaduct) are compared with the wind tunnel data. The NMSE and FB were used to quantify the accuracy of the simulation results. The metrics were computed using Eq. (13) and Eq. (14), where P_{WT} is the value of the wind tunnel experiment and P_S is the value of the simulation experiment. $-$ represents the average. As shown in Fig. 7 and Table 4, whether on the leeward or windward side, the NMSE and FB are within acceptable error limits, indicating that our simulations in this study are reasonable. "Salim" in Fig. 7 shows the simulation results of the LES in (Salim et al., 2011a). Except for the FB on the leeward side, the LES has a smaller error than does the RANS for both NMSEs. The performance metrics of LES are better than those of RANS.

$$NMSE = \frac{\overline{|P_{WT} - P_S|}}{\overline{P_{WT}}\,\overline{P_S}} \tag{13}$$

$$\mathrm{FB} = \frac{2(\overline{P_{WT}} - \overline{P_s})}{\overline{P_{WT}} + \overline{P_s}} \tag{14}$$

3. Results and Discussions

3.1. Turbulent Flow

In all the cases, the approaching wind with $v_H = 4.7\mathrm{m/s}$ is perpendicular to the canyon's central axis. In the canyon, there will be only one major vortex (Baik & Kim, 1999).

In this situation, the traffic pollutants carried by the vortex accumulate on the backside of the canyon, leading to high local concentrations. If a viaduct is erected in the canyon, the skimming regime may be destroyed. The 3D streamlines in the canyons at different viaduct heights h_v are shown in Fig. 8.

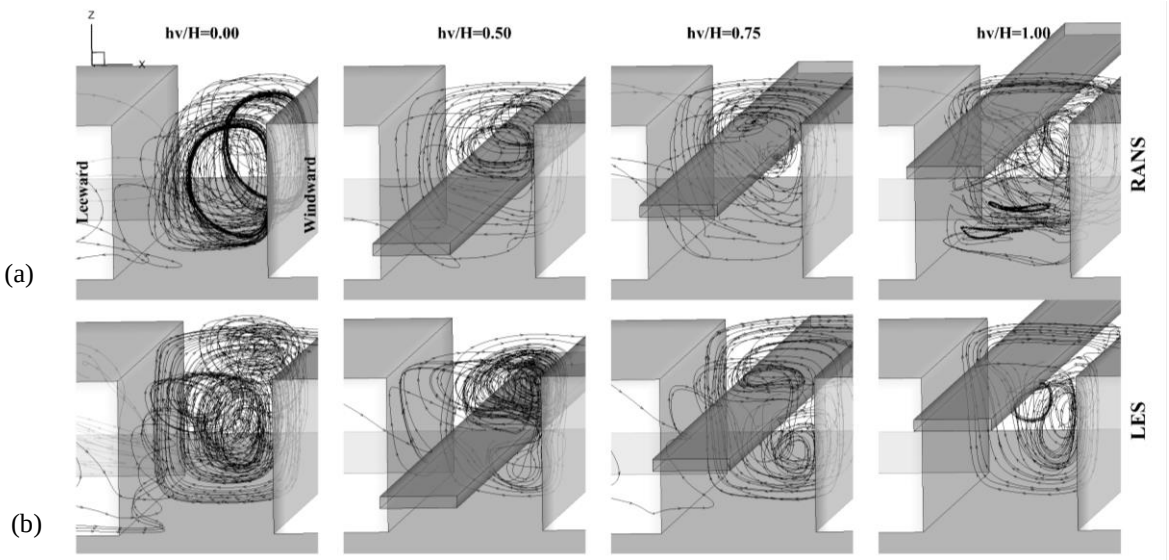

Fig. 8 3D streamlines in street canyons with viaducts at different heights h_v above the ground: comparison between (a) RANS results and (b) LES results

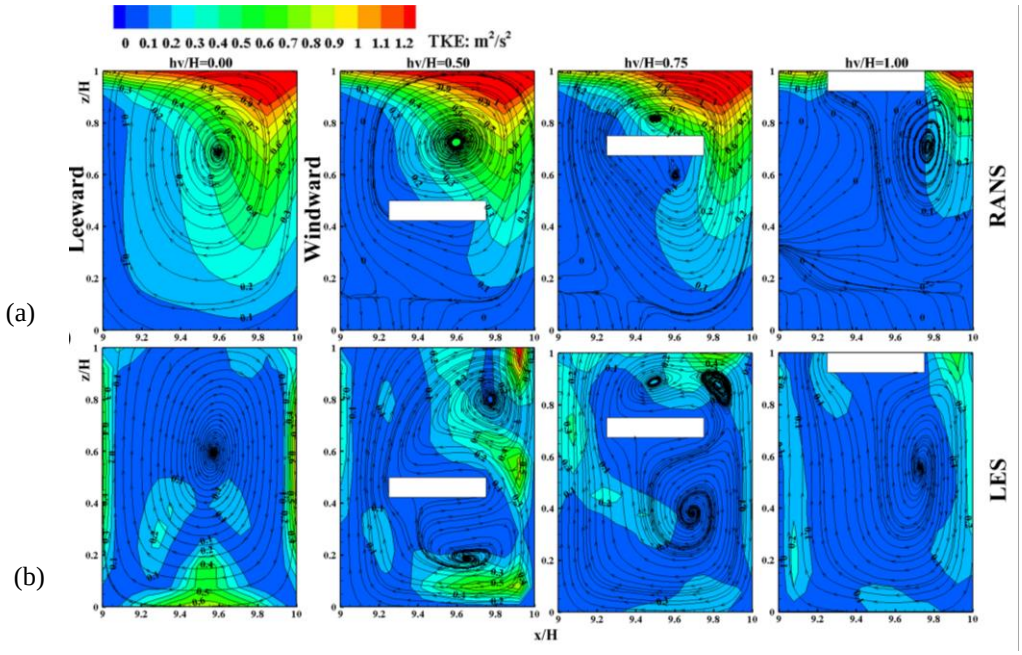

Fig. 5 Distributions of TKE and flow visualization (time-averaged data) at the mid-plane of the canyon (y/H=0 and x/H=9-10): comparison between the (a) RANS results and (b) LES results

The RANS results are presented in Fig. 8(a), in which a single main vortex is found inside the canyon without a viaduct ($h_v/H = 0$). When a viaduct is erected ($h_v/H > 0$), only one strong vortex surrounding the viaduct is observed for different h_v/H, which is consistent with the RANS results obtained by (Hang et al., 2017; He et al., 2017) for 3D canyons with similar aspect ratios. However, in the 2D street canyon studied by (Zhang et al., 2012), two strong vortices formed in the canyon when the viaduct was placed at $h_v/H = 0.5$. The difference between the 2D and 3D cases may have occurred because a 3D canyon with finite length cannot be completely regarded as an ideal 2D canyon. However, in the LES results presented in Fig. 8(b), a similar flow regime as that in the RANS case without a viaduct was observed, as expected. Nevertheless, the single main vortex is split by the viaduct into two vortices when $0 < h_v/H < 1$, which are quite different from those in the RANS cases. Therefore, the LES cases in this study are more reasonable than the RANS cases, implying that the RANS methods fail to ensure the accuracy of predictions of the flow regime within canyons with a viaduct. Lastly, when the viaduct is erected at the roof of the canyons ($h_v/H = 1$), the flow above the viaduct is directly affected by the ambient wind, and only one strong vortex is formed under the viaduct.

The TKE is the key variable in the micro-atmospheric environment for measuring the intensity of turbulence. It is made with $k = \frac{1}{2}\left(\overline{u'^2} + \overline{v'^2} + \overline{w'^2}\right)$, where $u_i' = u_i - \overline{u_i}$ is the velocity fluctuation. It has been verified that the agreement of the TKE between the measurement data and LES is better than that for the RANS (van Hooff et al., 2017). Figure 9 presents the TKE and flow visualization in the mid-plane ($y/H = 0$) of the canyon.

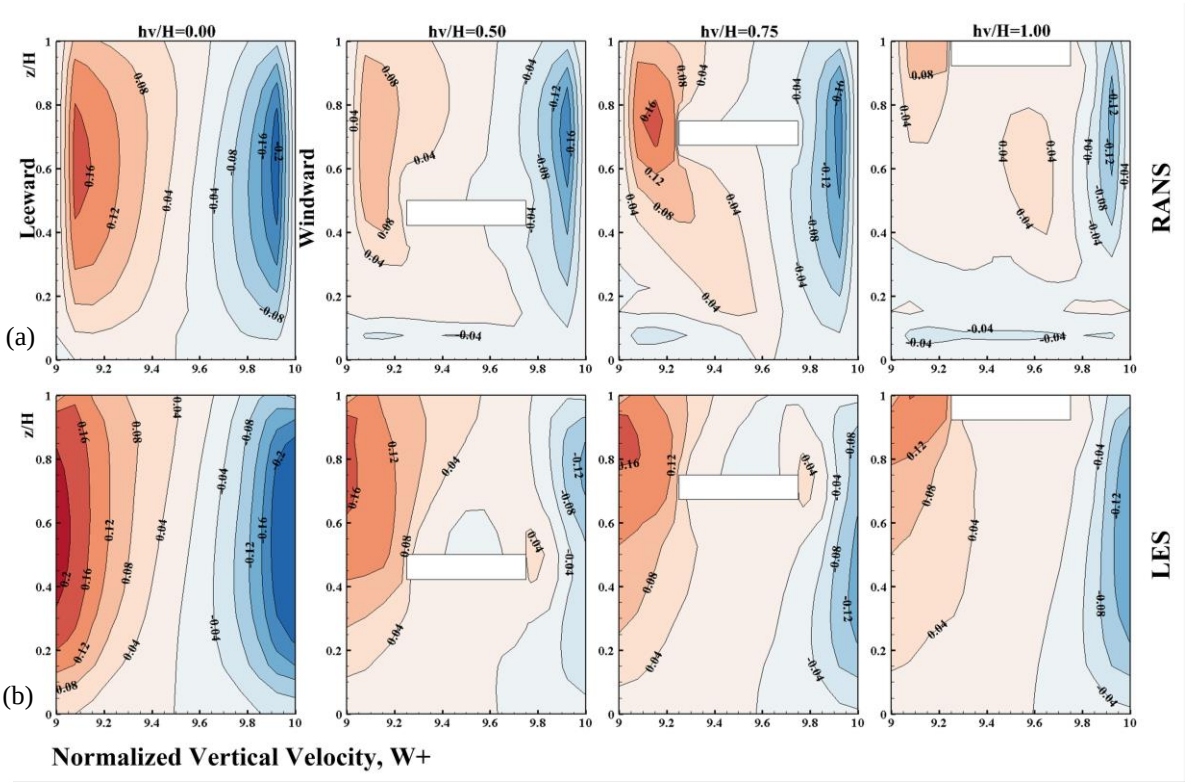

Fig. 6 Mean normalized vertical velocity contours at the mid-plane of the canyon (y/H=0 and x/H ranges from 9 to 10) of the street canyons with viaducts at different heights h_v above the ground: comparison between (a) the RANS results and (b) LES results

Since small-scale turbulence is captured by LES cases, LES shows more realistic results compared with the hierarchical distribution of k in RANS cases, and the value of k given by LES is larger than that of RANS in the region underneath a viaduct and the leeward facade, while the opposite pattern occurs above the viaduct.

These results indicate that the momentum diffusion was underestimated by the RANS method. As the viaduct height increases, both the RANS and LES models indicate that the TKE underneath the viaduct decreases. Based on the LES results, the presence of a viaduct reduces the TKE at the bottom of the leeward facade. The maximum value of k beneath the viaduct can still exceed $0.5m^2/s^2$ on the windward side when the height of the viaduct is set to $0.5H$. Similarly, at $0.6H$ (slightly above the viaduct), clockwise vortices are observed near both locations. In cases 7 and 8, the heights of the viaduct are set to 0.75H and 1.00H, the k underneath the viaduct ranges from $0 \sim 0.2m^2/s^2$, and the center of the clockwise vortex generated underneath the viaduct moves toward the windward side as the height of the viaduct increases. Moreover, k always had a maximum value on the leeward/windward sides at the same height as that of the viaduct. This finding implies that the presence of a viaduct in a canyon strengthens the turbulence transmission near the viaduct.

In Fig. 6, the mean velocity is calculated using $w^+ = u(z)/u(H)$, where u(H) is the free-stream velocity. Both RANS and LES captured only one main vortex when $h_v/H = 0$ and $h_v/H = 1$, and LES revealed more vortices underneath the viaduct when $0 < H_v/H < 1$.

Fig. 6 graphically presents the mean normalized vertical velocity contours at the mid-plane of the canyons. Generally, in all cases, RANS underpredicted the maximum vertical velocity compared to LES. In cases without a viaduct, both RANS and LES form two obvious vertical velocity cores, and the maximum normalized vertical velocity magnitude is 0.2, indicating that the results are quite similar. The vertical velocity contours in the RANS cases show that small negative values ($0 \sim -0.04\mathrm{m/s}$) were observed near the ground.

In addition, the location of the largest vertical velocity on the leeward side changes with the height of the viaduct in both the LES and RANS cases. The vertical velocities in the whole street canyon are reduced by the viaducts, which weakens the dispersion of pollutants underneath the viaducts.

3.2. Pollutant Concentration

The impact of the viaduct settings on the pollutant concentration within the canyons is given in this section as well as a comparison between RANS and LES. The presence of a viaduct changes the structure of the flow field within the canyons, and the maximum vertical velocities were found at the height of the viaduct. The gaseous pollutant used in this study is the inert gas SF_6. Thus, there is no chemical reaction involved in our simulations. The pollutant disperses under the advection diffusion of the mean flow and the mixing process of the turbulent fluctuations. However, viaducts change the flow regime within street canyons and affect the distribution of air pollutants.

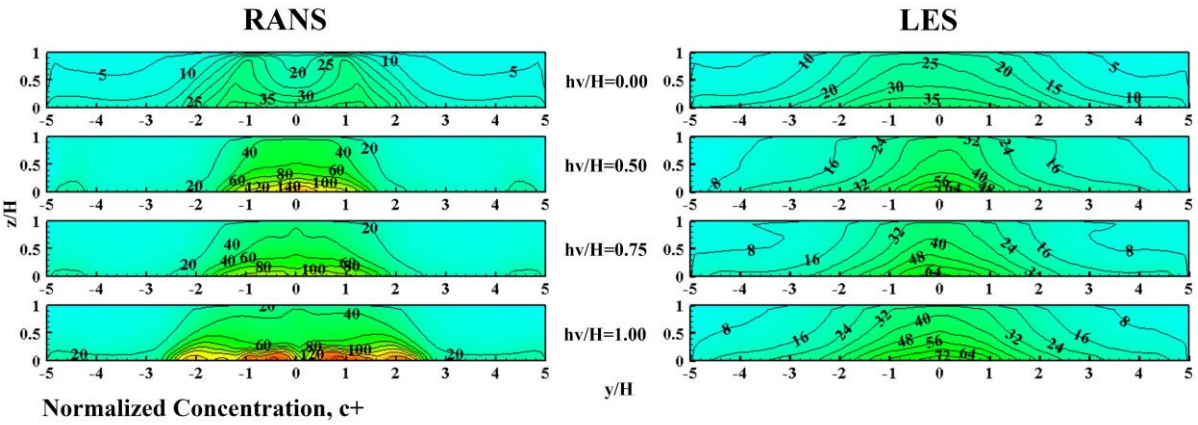

Fig. 7 Mean normalized concentration contours at the leeward façades of street canyons with viaducts at different heights h_v above the ground: comparison between the (a) RANS results and (b) LES results

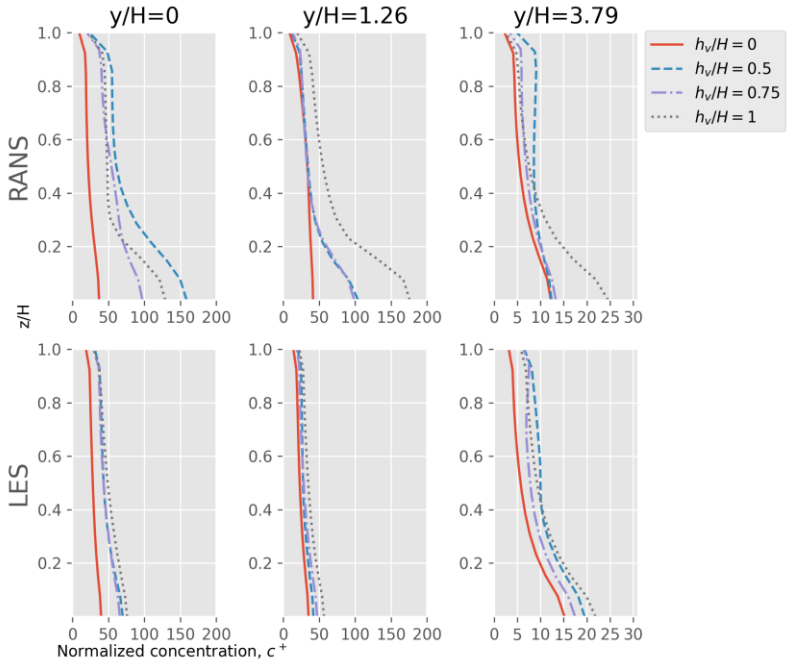

Fig. 8 Mean normalized concentration profiles at three different locations (y/H=0, 1.26 and 3.79) on the leeward side

In this section, the impacts of viaduct settings on the flow and air pollutant dispersion will be investigated, and a comparison between LES and RANS will be discussed. The mean normalized concentrations of the leeward facades of the canyons are presented in Fig. 7, and the concentration profiles at three locations (y/H=0, 1.26 and 3.79) were selected to determine the detailed concentration distributions in the vertical direction.

Generally, the concentrations obtained from RANS models are mostly M-shaped in the y-plane, as shown in Fig. 7. RANS tends to underestimate the accumulation of pollutants in the middle of the canyon, while the LES results show the maximum pollutant concentration in this location. The tendency of RANS to show a smaller concentration than LES on a horizontal section was also observed in a previous study. This phenomenon illustrates the necessities of performing the analysis on the horizontal plane along the street canyon.

Further observations from Fig. 8 imply that the maximum concentration obtained from the RANS on the leeward facade is nearly twice as high as that of the LES results at the middle plane (y/H=0). This result reflects that RANS underestimated the vertical velocity on the leeward side, resulting in an overprediction of pollutant accumulation. Based on the LES results, compared to the cases without a viaduct, the maximum concentration on the leeward side increases from 39.76 (h_v/H=0) to 69.80 (h_v/H=0.5), 65.79 (h_v/H=0.75), and 75.97 (h_v/H=1), increasing by 75.55%, 65.47%, and 91.07%, respectively. When the viaduct height is 0.75H in case 7, it showed the best ventilation efficiency compared with the other cases with a viaduct, leading to the maximum pollutant

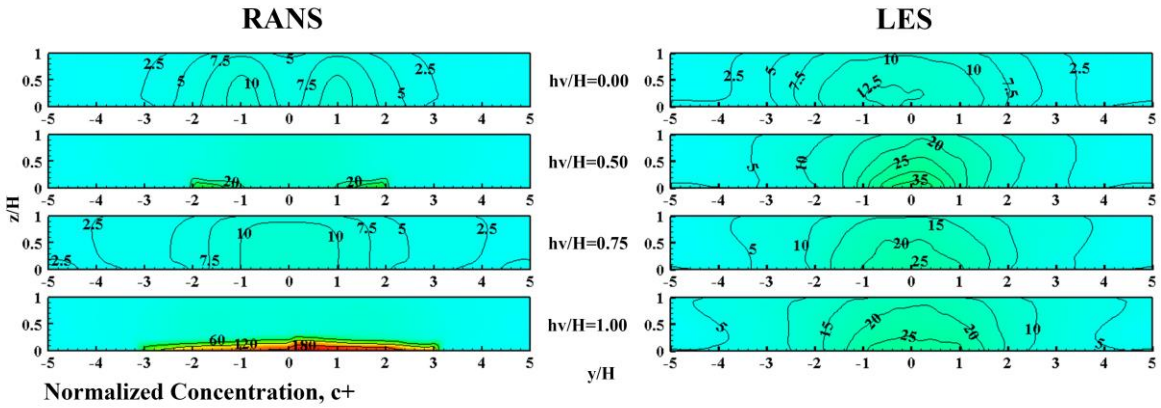

Fig. 9 Mean normalized concentration contours at the windward façades of street canyons with viaducts at different heights h_v above the ground: comparison between the (a) RANS results and (b) LES results

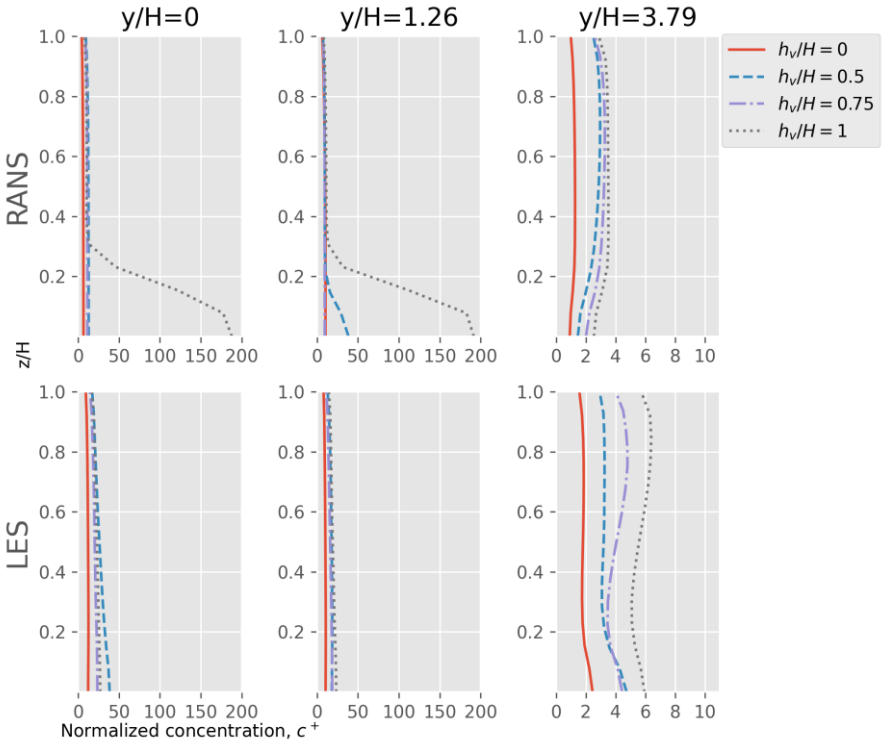

Fig. 10 Mean normalized concentration profiles at three different locations (y/H=0, 1.26 and 3.79) on the windward sides

concentration on the leeward side being lower than that in the other LES cases. An increase or decrease in the viaduct height has a weak impact on the pollution concentration, with a fluctuation within 15% but exceeding 50% in the RANS cases.

As shown in Fig. 9 and Fig. 10 , it is necessary to note that RANS predicted more than 6 times the concentration compared to LES on the windward façade when the viaduct was abreast with the roof of the building ($h_v/H = 1$). In case 4, pollutants accumulated most heavily at the bottom of the canyon because RANS predicts low vertical velocities and TKE at the bottom of the canyon. Fig. 11 and 13 showed that pollutant accumulation occurs on both the windward and leeward sides. However, in case 8, higher TKE and vertical velocities were clearly observed compared to case 4, so the LES predicted lower concentrations in the canyon.

In other cases, the predictions from RANS are approximately twice those of the LES. The reasons for these significant discrepancies are that when the viaduct is abreast with the roof ($h_v/H = 1$), the ventilation underneath the canyon is extremely poor, and small-scale horizontal vortices are formed (see Fig. 8(a)) near the ground, which hinders the removal of pollutants. Moreover, for street canyons with a viaduct, both RANS and LES showed that $h_v/H = 0.75$ predicted lower concentrations than the others.

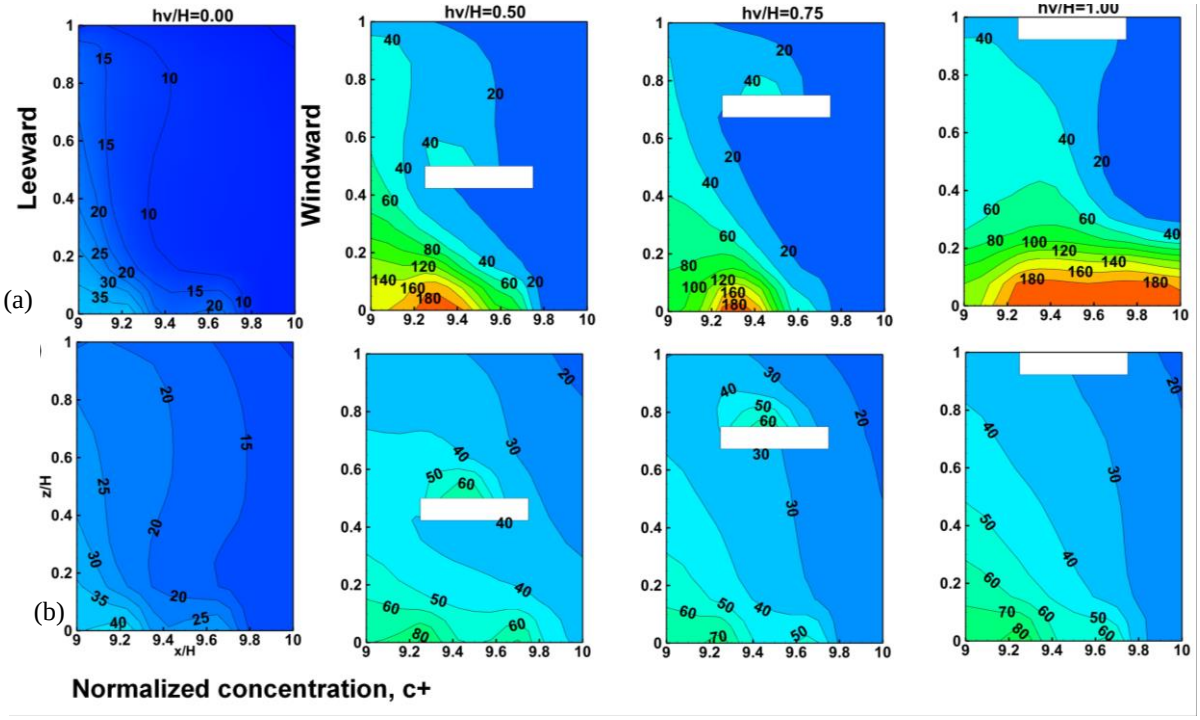

Fig. 11 Mean normalized concentration contours at the mid-plane (y/H=0 and x/H=9-10) of the street canyons with viaducts at different heights h_v above the ground: comparison between the (a) RANS results and (b) LES results

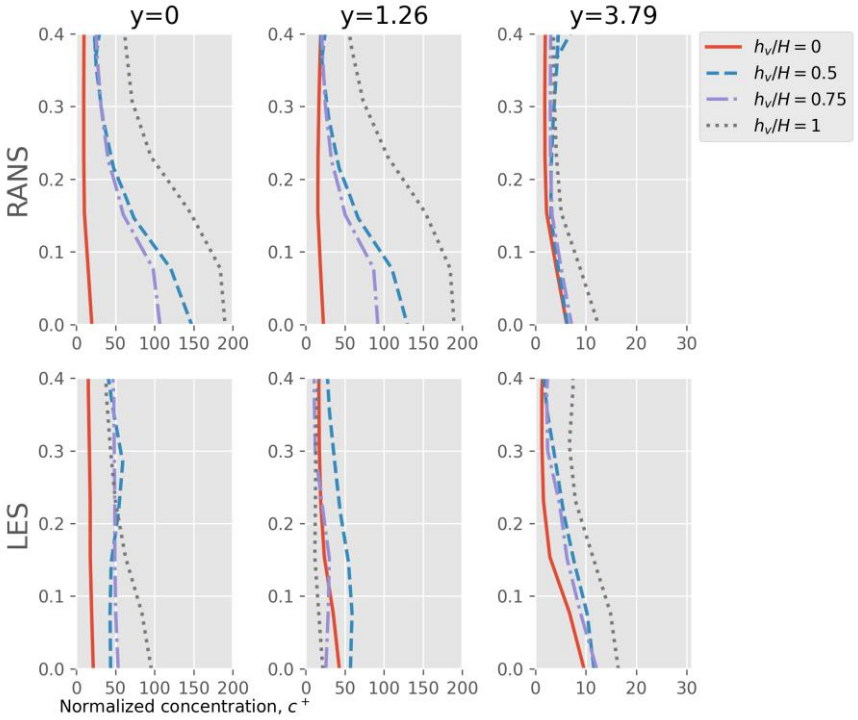

Fig. 12 Mean normalized concentration profiles at three different locations (y/H=0, 1.26 and 3.79) in the central plane of the street canyon

Fig. 11 illustrates the mean normalized concentrations at the mid-plane of the canyons. In cases without a viaduct, the distribution of pollutants in RANS is similar to that in LES, as expected, owing to their similar flow fields.

However, RANS significantly overestimates the concentration when a viaduct is erected. Moreover, the main location of most pollutant accumulation predicted by the two models shows no difference, but LES revealed a subregion of pollutant accumulation above the ground. In fact, these locations correspond exactly to the location where the emission source is located, which further reflects the accuracy of the LES predictions. Fig. 12 plots the mean normalized concentration profiles below 0.4H at three different locations (y/H=0, 1.26 and 3.79) in the vertical central plane of the street canyon (x/H=9.50).

Both RANS and LES imply that the accumulation of pollutants becomes more severe from $z/H = 0.15$ to the ground. At the ends of the canyon, where pollutants are easily removed by external flow (y/H=3.79), the predictions of the two models for pollutants are similar, which demonstrates that in regions with better ventilation, the predictions by RANS and LES may be consistent, while in regions with weak ventilation, LES is more accurate than RANS.

4. CONCLUSION

In this work, comprehensive comparisons between the simulation results of steady RANS (SKE) and LES (dynamic Smagorinsky SGS) in canyons with a viaduct were conducted to understand the impact of the viaduct settings on flow structures and air pollution. Four viaduct settings were considered: no viaduct, h_v/H=0.5, h_v/H=0.75, and h_v/H=1.

The validation was based on the pollutant concentration in the vertical direction in the canyon without the viaduct. The validation shows that LES has less error than RANS. Without the viaduct, RANS predicted lower pollution concentrations in the y/H=0 plane than in the wind tunnel. Further detailed analysis was performed based on the simulation results. When different viaduct heights are taken into account, both the RANS and LES results show higher pollution concentrations. The presence of a viaduct deteriorates ventilation in canyons. LES is able to capture the complex flow structure within a canyon with a viaduct, while RANS fails to predict the two-vortex flow regime in cases with $h_v/H = 0.5$ and 0.75. Both RANS and LES predicted minimal pollution concentrations at $h_v/H = 0.75$ near the ground. In the region below z/H = 0.4, RANS predicted higher concentrations than LES, and the results all showed contamination accumulation. LES can capture more detailed flow structures due to the reproduction of transient concentration features in canyons, such as small-scale vortices in canyons, and therefore performs better than steady RANS models. Despite the change in the viaduct height, both RANS and LES imply that the accumulation of pollutants becomes more severe from z/H=0.15 to the ground when a viaduct is built, and the "necking effect" is found in the region on the leeward/windward side wall at the height of the viaduct level, where the vertical velocity always has the maximum positive/negative values.

These comparisons are crucial when deciding which numerical method to use and to help in drafting guidelines for analysis and optimization within a canyon scene. The discussion about the impact of different viaduct height settings on air pollutant dispersion can help to analyze the causes of pollution in traffic microenvironments.

ACKNOWLEDGEMENTS

This work was supported by the [National Natural Science Foundation of China] under Grant [number 41975165, 11802347]; [Science and Technology Planning Project of Guangdong Province] under Grant [number 2023B1212060029]. The authors would like to express sincere thanks to Dr. Christof Gromke for his experimental data supply.

CONFLICT OF INTEREST

No potential conflict of interest was reported by the authors.

AUTHORS CONTRIBUTION

R. Xu: Conceptualization; Methodology; Numerical computation & analysis; Writing-original draft. **T. Chen:** Conceptualization; Writing-original draft; Methodology; Numeral analysis. **Y. X. Fu:** Conceptualization; Writing-original draft. **J. C. Chen:** Conceptualization; Funding acquisition; Methodology; Discussion; Review & editing. **Y. H. Liu:** Conceptualization; Funding acquisition; Review & editing.

REFERENCES

Allegrini, J. (2018). A wind tunnel study on three-dimensional buoyant flows in street canyons with different roof shapes and building lengths. *Building and Environment*, *143*, 71–88. https://doi.org/10.1016/j.buildenv.2018.06.056

Baik, J. J., & Kim, J. J. (1999). A Numerical study of flow and pollutant dispersion characteristics in urban street canyons. *Journal of Applied Meteorology and Climatology*, *38*(11), 1576–1589. https://doi.org/10.1175/1520-0450(1999)038<1576:ANSOFA>2.0.CO;2

Bouarbi, L., Abed, B., & Bouzit, M. (2016). Computational analysis of pollutant dispersion in urban street canyons with tree planting influenced by building roof shapes. *Wind and Structures*, *23*(6), 505–521. https://doi.org/10.12989/was.2016.23.6.505

Breuer, M., Jovičić, N., & Mazaev, K. (2003). Comparison of DES, RANS and LES for the separated flow around a flat plate at high incidence. *International Journal for Numerical Methods in Fluids*, *41*(4), 357–388. https://doi.org/10.1002/fld.445

Chang, C. H., & Meroney, R. N. (2003). Concentration and flow distributions in urban street canyons: Wind tunnel and computational data. *Journal of Wind Engineering and Industrial Aerodynamics*, *91*(9), 1141–1154. https://doi.org/10.1016/S0167-6105(03)00056-4

Chatzimichailidis, A. E., Argyropoulos, C. D., Assael, M. J., & Kakosimos, K. E. (2019). Qualitative and quantitative investigation of multiple large eddy simulation aspects for pollutant dispersion in street canyons using OpenFOAM. *Atmosphere*, *10*(1). https://doi.org/10.3390/atmos10010017

Chew, L. W., Aliabadi, A. A., & Norford, L. K. (2018a). Flows across high aspect ratio street canyons:

Reynolds number independence revisited. *Environmental Fluid Mechanics*, *18*(5), 1275–1291. https://doi.org/10.1007/s10652-018-9601-0

Chew, L. W., Glicksman, L. R., & Norford, L. K. (2018b). Buoyant flows in street canyons: Comparison of RANS and LES at reduced and full scales. *Building and Environment*, *146*, 77–87. https://doi.org/10.1016/j.buildenv.2018.09.026

Ding, S., Huang, Y., Cui, P., Wu, J., Li, M., & Liu, D. (2019). Impact of viaduct on flow reversion and pollutant dispersion in 2D urban street canyon with different roof shapes—Numerical simulation and wind tunnel experiment. *Science of The Total Environment*, *671*, 976–991. https://doi.org/10.1016/j.scitotenv.2019.03.391

Eliasson, I., Offerle, B., Grimmond, C. S. B., & Lindqvist, S. (2006). Wind fields and turbulence statistics in an urban street canyon. *Atmospheric Environment*, *40*(1), 1–16. https://doi.org/10.1016/j.atmosenv.2005.03.031

Gousseau, P., Blocken, B., Stathopoulos, T., & van Heijst, G. J. F. (2011). CFD simulation of near-field pollutant dispersion on a high-resolution grid: A case study by LES and RANS for a building group in downtown Montreal. *Atmospheric Environment*, *45*(2), 428–438. https://doi.org/10.1016/j.atmosenv.2010.09.065

Gromke, C. B. (2013). A database for the validation of street canyon dispersion models. *Proceedings of the 15th International Conference on Harmonisation within Atmospheric Dispersion Modelling for Regulatory Purposes* (HARMO), May 6-9, 2013, Madrid, Spain. https://research.tue.nl/en/publications/codasc-a-database-for-the-validation-of-street-canyon-dispersion-

Gromke, C., & Ruck, B. (2007). Influence of trees on the dispersion of pollutants in an urban street canyon-Experimental investigation of the flow and concentration field. *Atmospheric Environment*, *41*(16), 3287–3302. https://doi.org/10.1016/j.atmosenv.2006.12.043

Gromke, C., & Ruck, B. (2009). On the impact of trees on dispersion processes of traffic emissions in street canyons. *Boundary-Layer Meteorology*, *131*(1), 19–34. Scopus. https://doi.org/10.1007/s10546-008-9301-2

Gu, Z. L., Zhang, Y. W., Cheng, Y., & Lee, S. C. (2011). Effect of uneven building layout on air flow and pollutant dispersion in non-uniform street canyons. *Building and Environment*, *46*(12), 2657–2665. https://doi.org/10.1016/j.buildenv.2011.06.028

Hang, J., Buccolieri, R., Yang, X., Yang, H., Quarta, F., & Wang, B. (2019). Impact of indoor-outdoor temperature differences on dispersion of gaseous pollutant and particles in idealized street canyons with and without viaduct settings. *Building Simulation*, *12*(2), 285–297. Scopus. https://doi.org/10.1007/s12273-018-0476-2

Hang, J., Li, Y., Sandberg, M., Buccolieri, R., & Di Sabatino, S. (2012). The influence of building height variability on pollutant dispersion and pedestrian ventilation in idealized high-rise urban areas. *Building and Environment*, *56*, 346–360. Scopus. https://doi.org/10.1016/j.buildenv.2012.03.023

Hang, J., Lin, M., Wong, D. C., Wang, X., Wang, B., & Buccolieri, R. (2016). On the influence of viaduct and ground heating on pollutant dispersion in 2D street canyons and toward single-sided ventilated buildings. *Atmospheric Pollution Research*, *7*(5), 817–832. Scopus. https://doi.org/10.1016/j.apr.2016.04.009

Hang, J., Luo, Z., Wang, X., He, L., Wang, B., & Zhu, W. (2017). The influence of street layouts and viaduct settings on daily carbon monoxide exposure and intake fraction in idealized urban canyons. *Environmental Pollution*, *220*, 72–86. https://doi.org/10.1016/j.envpol.2016.09.024

Hang, J., Xian, Z., Wang, D., Mak, C. M., Wang, B., & Fan, Y. (2018). The impacts of viaduct settings and street aspect ratios on personal intake fraction in three-dimensional urban-like geometries. *Building and Environment*, *143*, 138–162. Scopus. https://doi.org/10.1016/j.buildenv.2018.07.001

Hayati, A. N., Stoll, R., Pardyjak, E. R., Harman, T., & Kim, J. J. (2019). Comparative metrics for computational approaches in non-uniform street-canyon flows. *Building and Environment*, *158*, 16–27. https://doi.org/10.1016/j.buildenv.2019.04.028

He, L., Hang, J., Wang, X., Lin, B., Li, X., & Lan, G. (2017). Numerical investigations of flow and passive pollutant exposure in high-rise deep street canyons with various street aspect ratios and viaduct settings. *Science of the Total Environment*, *584-585*, 189–206. https://doi.org/10.1016/j.scitotenv.2017.01.138

Huang, X., Wang, H., & Gao, L. (2023). Numerical simulation of airflow and dispersion in 3D street canyons: The effect of atmospheric temperature stratification. *Environmental Technology*, *44*(17), 2563–2580. https://doi.org/10.1080/09593330.2022.2036247

Jon, K. S., Huang, Y., Sin, C. H., Cui, P., & Luo, Y. (2023a). Influence of wind direction on the ventilation and pollutant dispersion in different 3D street canyon configurations: Numerical simulation and wind-tunnel experiment. *Environmental Science and Pollution Research*, *30*(11), 31647–31675. https://doi.org/10.1007/s11356-022-24212-0

Jon, K. S., Luo, Y., Sin, C. H., Cui, P., Huang, Y., & Tokgo, J. (2023b). Impacts of wind direction on the ventilation and pollutant dispersion of 3D street canyon with balconies. *Building and Environment*, *230*, 110034. https://doi.org/10.1016/j.buildenv.2023.110034

Joerger, V. M., & Pryor, S. C. (2018). Ultrafine particle number concentrations and size distributions around an elevated highway viaduct. *Atmospheric Pollution*

Research, *9*(4), 714–722. https://doi.org/10.1016/j.apr.2018.01.008

Kastner-Klein, P., & Plate, E. J. (1999). Wind-tunnel study of concentration fields in street canyons. *Atmospheric Environment*, *33*(24), 3973–3979. https://doi.org/10.1016/S1352-2310(99)00139-9

Kikumoto, H., & Ooka, R. (2012). A study on air pollutant dispersion with bimolecular reactions in urban street canyons using large-eddy simulations. *Journal of Wind Engineering and Industrial Aerodynamics*, *104–106*, 516–522. https://doi.org/10.1016/j.jweia.2012.03.001

Kim, K. H., Kabir, E., & Kabir, S. (2015). A review on the human health impact of airborne particulate matter. *Environment International*, *74*, 136–143. https://doi.org/10.1016/j.envint.2014.10.005

Kumar, P., Garmory, A., Ketzel, M., Berkowicz, R., & Britter, R. (2009). Comparative study of measured and modelled number concentrations of nanoparticles in an urban street canyon. *Atmospheric Environment*, *43*(4), 949–958. https://doi.org/10.1016/j.atmosenv.2008.10.025

Li, X. X., Liu, C. H., & Leung, D. Y. C. (2008). Large-eddy simulation of flow and pollutant dispersion in high-aspect-ratio urban street canyons with wall model. *Boundary-Layer Meteorology*, *129*(2), 249–268. https://doi.org/10.1007/s10546-008-9313-y

Li, X.-X., Liu, C.-H., Leung, D. Y. C., & Lam, K. M. (2006). Recent progress in CFD modelling of wind field and pollutant transport in street canyons. *Atmospheric Environment*, *40*(29), 5640–5658. https://doi.org/10.1016/j.atmosenv.2006.04.055

Li, X.-X., Britter, R., & Norford, L. K. (2016). Effect of stable stratification on dispersion within urban street canyons: A large-eddy simulation. *Atmospheric Environment*, *144*, 47–59. https://doi.org/10.1016/j.atmosenv.2016.08.069

Li, Z., Cai, C., Huang, X., Dou, H., Fang, W., & Ming, T. (2018). Numerical simulation on the effect of viaduct settings on the air flow and pollutants dispersion in the deep street canyon. *Research of Environmental Sciences*, *31*(2), 254–264. https://doi.org/10.13198/j.issn.1001-6929.2017.03.73

Liu, Y., Ding, H., Chang, S., Lu, R., Zhong, H., Zhao, N., Lin, T. H., Bao, Y., Yap, L., Xu, W., Wang, M., Li, Y., Qin, S., Zhao, Y., Geng, X., Wang, S., Chen, E., Yu, Z., Chan, T. C., & Liu, S. (2020). Exposure to air pollution and scarlet fever resurgence in China: A six-year surveillance study. *Nature Communications*, *11*(1), https://doi.org/10.1038/s41467-020-17987-8

Llaguno-Munitxa, M., Bou-Zeid, E., & Hultmark, M. (2017). The influence of building geometry on street canyon air flow: Validation of large eddy simulations against wind tunnel experiments. *Journal of Wind Engineering and Industrial Aerodynamics*, *165*, 115–130. https://doi.org/10.1016/j.jweia.2017.03.007

Longo, R., Bellemans, A., Derudi, M., & Parente, A. (2020). A multi-fidelity framework for the estimation of the turbulent Schmidt number in the simulation of atmospheric dispersion. *Building and Environment*, *185*, 107066. https://doi.org/10.1016/j.buildenv.2020.107066

Mei, S. J., Luo, Z., Zhao, F. Y., & Wang, H. Q. (2019). Street canyon ventilation and airborne pollutant dispersion: 2-D versus 3-D CFD simulations. *Sustainable Cities and Society*, *50*, 101700. https://doi.org/10.1016/j.scs.2019.101700

Meroney, R. N., Pavageau, M., Rafailidis, S., & Schatzmann, M. (1996). Study of line source characteristics for 2-D physical modelling of pollutant dispersion in street canyons. *Journal of Wind Engineering and Industrial Aerodynamics*, *62*(1), 37–56. https://doi.org/10.1016/S0167-6105(96)00057-8

Ming, T., Nie, C., Li, W., Kang, X., Wu, Y., Zhang, M., & Peng, C. (2022). Numerical study of reactive pollutants diffusion in urban street canyons with a viaduct. *Building Simulation*, *15*(7), 1227–1241. https://doi.org/10.1007/s12273-021-0795-6

Moonen, P., Gromke, C., & Dorer, V. (2013). Performance assessment of Large Eddy Simulation (LES) for modeling dispersion in an urban street canyon with tree planting. *Atmospheric Environment*, *75*, 66–76. https://doi.org/10.1016/j.atmosenv.2013.04.016

Ng, W. -Y., & Chau, C.-K. (2014). A modeling investigation of the impact of street and building configurations on personal air pollutant exposure in isolated deep urban canyons. *Science of The Total Environment*, *468–469*, 429–448. https://doi.org/10.1016/j.scitotenv.2013.08.077

Nguyen, V. T., Nguyen, T. C., & Nguyen, J. (2019). Numerical simulation of turbulent flow and pollutant dispersion in urban street canyons. *Atmosphere*, *10*(11). https://doi.org/10.3390/atmos10110683

Pu, Y., & Yang, C. (2014). Estimating urban roadside emissions with an atmospheric dispersion model based on in-field measurements. *Environmental Pollution*, *192*, 300–307. https://doi.org/10.1016/j.envpol.2014.05.019

Oachim & Ichhorn (2004). *Simulation of effects of vegetation on the dispersion of pollutants in street canyons.* https://www.semanticscholar.org/paper/Simulation-of-effects-of-vegetation-on-the-of-in-Oachim-Ichhorn/9d91b7d7bdfc0ea930cc4a5963cd7b5e3e88e943

Qin, C., Song, C., Wang, S., & Zhao, J. (2018). Numerical study on the air environment of ideal street valley with double viaduct in vertical windward. *Huanjing Kexue Xuebao/Acta Scientiae Circumstantiae*, *38*(9), 3467–3474. https://doi.org/10.13671/j.hjkxxb.2018.0154

Rossi, R., & Iaccarino, G. (2009). Numerical simulation of scalar dispersion downstream of a square obstacle using gradient-transport type models. *Atmospheric Environment*, *43*(16), 2518–2531. https://doi.org/10.1016/j.atmosenv.2009.02.044

Salim, S. M., & Ong, K. C. (2013). Performance of RANS, URANS and LES in the prediction of airflow and pollutant dispersion. In H. K. Kim, S. I. Ao, & B. B. Rieger (Eds.), *IAENG transactions on engineering technologies: Special edition of the world congress on engineering and computer science 2011* (pp. 263–274). Springer Netherlands. https://doi.org/10.1007/978-94-007-4786-9_21

Salim, S. M., Buccolieri, R., Chan, A., & Di Sabatino, S. (2011a). Numerical simulation of atmospheric pollutant dispersion in an urban street canyon: Comparison between RANS and LES. *Journal of Wind Engineering and Industrial Aerodynamics*, *99*(2–3), 103–113. https://doi.org/10.1016/j.jweia.2010.12.002

Salim, S. M., Cheah, S. C., & Chan, A. (2011b). Numerical simulation of dispersion in urban street canyons with avenue-like tree plantings: Comparison between RANS and LES. *Building and Environment*, *46*(9), 1735–1746. https://doi.org/10.1016/j.buildenv.2011.01.032

Shao, J., & Zhang, C. (2006). Numerical analysis of the flow around a circular cylinder using RANS and LES. *International Journal of Computational Fluid Dynamics*, *20*(5), 301–307. https://doi.org/10.1080/10618560600898437

So, E. S. P., Chan, A. T. Y., & Wong, A. Y. T. (2005). Large-eddy simulations of wind flow and pollutant dispersion in a street canyon. *Atmospheric Environment*, *39*(20), 3573–3582. https://doi.org/10.1016/j.atmosenv.2005.02.044

Takano, Y., & Moonen, P. (2013). On the influence of roof shape on flow and dispersion in an urban street canyon. *Journal of Wind Engineering and Industrial Aerodynamics*, *123*, 107–120. https://doi.org/10.1016/j.jweia.2013.10.006

Tominaga, Y., & Stathopoulos, T. (2013). CFD simulation of near-field pollutant dispersion in the urban environment: A review of current modeling techniques. *Atmospheric Environment*, *79*, 716–730. https://doi.org/10.1016/j.atmosenv.2013.07.028

Toparlar, Y., Blocken, B., Maiheu, B., & van Heijst, G. J. F. (2017). A review on the CFD analysis of urban microclimate. *Renewable and Sustainable Energy Reviews*, *80*, 1613–1640. https://doi.org/10.1016/j.rser.2017.05.248

van Hooff, T., Blocken, B., & Tominaga, Y. (2017). On the accuracy of CFD simulations of cross-ventilation flows for a generic isolated building: Comparison of RANS, LES and experiments. *Building and Environment*, *114*, 148–165. https://doi.org/10.1016/j.buildenv.2016.12.019

Wong, C. C. C., & Liu, C. H. (2014). Large-eddy simulation of flows over two-dimensional idealised street canyons with height variation. *International Journal of Environment and Pollution*, *54*(2/3/4), 147. https://doi.org/10.1504/IJEP.2014.065115

Zhang, C., Wen, M., Zeng, J., Zhang, G., Fang, H., & Li, Y. (2012). Modeling the impact of the viaduct on particles dispersion from vehicle exhaust in street canyons. *Science China Technological Sciences*, *55*(1), 48–55. https://doi.org/10.1007/s11431-011-4610-y

Zhang, K., Chen, G., Wang, X., Liu, S., Mak, C. M., Fan, Y., & Hang, J. (2019). Numerical evaluations of urban design technique to reduce vehicular personal intake fraction in deep street canyons. *Science of the Total Environment*, *653*, 968–994. https://doi.org/10.1016/j.scitotenv.2018.10.333

Zhang, Y., Gu, Z., & Yu, C. W. (2018). Review on numerical simulation of airflow and pollutant dispersion in urban street canyons under natural background wind condition. *Aerosol and Air Quality Research*, *18*(3), 780–789. https://doi.org/10.4209/aaqr.2017.09.0303

Zheng, X., & Yang, J. (2021). CFD simulations of wind flow and pollutant dispersion in a street canyon with traffic flow: Comparison between RANS and LES. *Sustainable Cities and Society*, *75*, 103307. https://doi.org/10.1016/j.scs.2021.103307

Zhou, B., Zhao, B., Guo, X., Chen, R., & Kan, H. (2013). Investigating the geographical heterogeneity in PM10-mortality associations in the china air pollution and health effects study (CAPES): A potential role of indoor exposure to PM10 of outdoor origin. *Atmospheric Environment*, *75*, 217–223. https://doi.org/10.1016/j.atmosenv.2013.04.044